Preparation, Characterization, and Performance Study of PVDF Nanocomposite Contained Hybrid Nanostructure TiO_2-POM Used as a Photocatalytic Membrane

Samadi Mollayousefi, Hamed; Fallah Shojaei, Abdollah*; Mahmoodi, Nosratollah *[+]

Department of Chemistry, University of Guilan, Rasht, I.R. IRAN

ABSTRACT: *In this work, polyvinylidene fluoride membranes were modified by introducing nanostructure TiO_2/SiO_2/POM hybrid fibers in the polymeric dope, to endow them with photocatalytic properties. For this purpose, initially, hybrid fibers were synthesized by electrospinning and calcination technique, and then these additives were incorporated into the membrane matrix. FT-IR and XRD analysis were used for the characterization of synthesized compounds. The FESEM manifests that the average diameter of the hybrid composite fibers is about 500 nm, and investigated membrane morphology. The properties of the prepared photocatalytic membrane were examined by several investigations such as pure water flux, contact angle, salt, and heavy metal rejection. Photocatalytic experiments confirm that membranes display a highly efficient and durable activity for the photodegradation of Methylene Bue (MB) and Humic Acid (HA). Experiments show that the prepared membranes have excellent stability under UV irradiation and can be used potentially for the separation of different components from water. The measurement accuracy and repeatability were determined by calculating the Standard Deviation and entered into Tables.*

KEYWORDS: *Hybrid nanostructure; Photocatalytic membrane; Polyoxometalate; Nanostructure TiO_2/SiO_2/POM hybrid fibers in the polymeric dope.*

INTRODUCTION

Increasing human activities in various fields, such as agriculture, livestock, and industry, lead to the entry of various organic and inorganic minerals into water, resulting in accumulation of contaminants including pigments, insecticides, antibodies, and heavy metals in the wastewater [1, 2]. The presence of these materials will cause severe damage to the environment and human health. Therefore, in recent years, special attention has been paid to eliminating these contaminants. Various strategies have been developed for this purpose, including physical, chemical and biological removal methods [3-6].

One of the techniques to eliminate pollution is to use catalysts that assist the process of more facile decomposition and removal of organic compounds, one of these compounds is TiO_2, which its photocatalytic activity has been investigated in various studies [7]. The TiO_2 is highly desirable because of its low cost, high chemical and oxidation stability, non-toxicity and efficient performance, while its wide bandgap and low photo-induced charge carrier's separation efficiency limits its application

** To whom correspondence should be addressed.*

+ E-mail: mahmoodi@guilan.ac.ir

1021-9986/2021/1/35-47 13/$/6.03

in practice[8]. Hence, many attempts have been made to eliminate TiO_2 defects in order to increase its catalytic efficiency [9,10]. For this purpose, generally, TiO_2 is used as composite forms with metals such as Ag, Au, Pt, etc. These conductive metals with a high ability to trap electrons in the visible wavelength increase the photocatalytic activity of TiO_2 [11-15]. However, composites, as mentioned earlier in addition to high prices, are unstable, in the photocatalytic process and cause the catalyst to be inactive [16].

Recently, polyoxometalates (POM) as a class of early transition metal-oxygen compounds have been attracted more attention due to their individual properties and controllable bandgap structure; therefore, these materials were presented as an appropriate solution to solve the above problem [17-19]. Due to the unique properties of polyoxometalates, it can be said that the simultaneous use of TiO_2 and POM can contribute to the absorption of light, and the photocatalytic properties of these two compounds are even better in the presence of the together [20]. So far, several studies about the POMs/TiO_2 composites have been reported, which have demonstrated better photocatalytic efficiency concerning that of TiO_2. However, there are some defects in this type of composites, such as the wide bandgaps of both POMs and TiO_2 [21-23]. In addition, due to the superior features of these types of photocatalysts, several researchers have used these smart catalysts in their reports.

For example, the development of photocatalysts in the membrane industry causes a boost in membrane performance. So that membranes containing photo-active nanoparticles can decompose the organic foulant to CO_2 and H_2O, and increase the efficiency of membranes in separating these compounds [24-26].

The Preparation of materials in the fiber form increases the surface-to-volume ratio and improves their catalytic activity. Electrospinning is the most common method for making nanofibers. Electrospinning has a significant advantage that includes cost-effectiveness, ease of use, and scalability. The repeatability, as well as the ability to produce long-length nanofibers, is another advantage of this method. To make inorganic nanofibers these materials are mixed with a polymer and used in the electrospinning process [27].

To the best of our knowledge, not much work has been reported on the incorporation of photocatalyst nanoparticles into the polymeric membranes. In the current study, hybrid mineral fibers were fabricated with TiO_2 and SiO_2 in the presence of POM and introduced into the membrane structure as an additive in order to create photocatalytic activity in the membrane. Molybdatophosphoric acid ($H_3PMo_{12}O_{40}$) were selected as the desired POM, and a facile electrospinning/calcination method were employed to fabricate $PMo_{12}/TiO_2/SiO_2$ hybrid nanofibers. Then, these nanofibers were incorporated into the poly (vinylidene fluoride) (PVDF) membrane matrix and were utilized as Mixed Matrix Membranes (MMM). Investigations show that these membranes have considerable photocatalytic properties in the elimination of soluble contaminations such as dyes and organic compounds. Besides, the characteristic properties of the prepared membranes have been investigated [28].

EXPERIMENTAL SECTION

Materials

Molybdatophosphoric acid ($H_3PMo_{12}O_{40}$), polyvinyl alcohol (PVA), methylene blue, and methyl orange were purchased from Merck Millipore. Poly (vinylidene fluoride) (PVDF), 1-methyl-2-pyrrolidinone (NMP, >99.5%), photocatalysts (TiO_2 <100 nm), SiO_2 (12 nm), deionized water was used throughout these experiments. Merck Millipore provided NaCl, $MgSO_4$ $ZnSO_4.7H_2O$, $Cd(NO_3)_2.4H_2O$ and different PEGs.

Preparation of MoPOM-TiO_2 nanofiber

The aqueous solution of PVA was prepared (5%wt) and MoPOM was added slowly into the solution and stirred vigorously until uniform yellowish mixture was obtained. This mixture was poured into a 10 mL syringe, and electrospinning was performed under the electrical potential of 15 kV. The electrode distance from the collector plate was 25 cm and the injection rate was about 0.5 mL/h. An aluminum foil was used as a collector, and the nanofibers collected on the foil were calcined at 500 °C for 5 hours to remove PVA.

Preparation of hybrid nanofiber

The procedure mentioned above, the desired amount of hybrid nanocomposite was added to the mixture before the electrospinning process and then nanofibers were fabricated and calcinated. (Table 1)

Table 1: Composition of polymeric dopes used in the spinning experiments.

Entry	PVA (g)	Additives (g)	Water [25]
1	0.5	0.1POM	10
2	0.5	0.1TiO_2	10
3	0.5	0.1POM + 0.1TiO_2	10
4	0.5	0.1POM + 0.1TiO_2 + 0.1SiO_2	10

Membrane Synthesis

Two wt.% of the additive as photocatalyst was added to the 1-methyl-2-pyrrolidinone (NMP) and dispersed ultrasonically for 30 minutes to obtain a perfectly uniform mixture. PEG 600 (10 wt.%) was combined with the mixture, and 20 wt.% of PVDF was gradually added to the mixture and stirred in a sealed container at 40°C for 24 hours to completely dissolve the polymer. The contents of the container were stirred ultrasonically again for 30 minutes, and a layer of a mixture with a thickness of 200 μm was spread on the surface of the smooth, clean glass plate, and immediately immersed in a coagulation non-solvent bath (distilled H_2O).

The films were kept inside the H_2O for 24 hours to complete the phase inversion process and the remaining solvent eliminates from the membranes. The membranes were removed from the H_2O and dried in a vacuum oven. The fabricated membranes were immersed in H_2O for 24 hours before use. The composition of polymeric dopes used in the membrane preparation is shown in Table 2.

Characterization

FT-IR spectra were acquired using a WQF-510A spectrophotometer in the range of 500–4000 cm-1 to analyze the functional groups. The spectra were recorded using the KBr pellet method. Field Emission Scanning Electron Microscope (FE-SEM) images were obtained to study the surface structure, cross-section and morphology of prepared nanocomposite membranes using HITACHI S-4160, operating 30kV. All samples were fractured in liquid nitrogen and then coated with a thin gold layer. Spectrophotometry studies were carried out using a UV spectrophotometer PG (China) with a 1cm quartz cell. The concentration of metal ions in the aqueous solutions was determined using a Shimadzu AA-670 atomic absorption spectrophotometer with a hollow cathode lamp was used an air–acetylene flame.

Molecular weight cut-off

Filtration test is performed to measure the Molecular Weight Cut Off (MWCO). For this purpose, a mixture of PEGs with different molecular weights ranging from 400 to 20000 g/mol with a total concentration of 5 g/L was used as the feed solution in the filtration cell, and the experimenting pressure was adjusted at 7 bar. Both feed and permeate solutions were analyzed by Gel Permeation Chromatography (GPC) (Knauer, Clean up unit 6500). The obtained chromatograms were integrated and set with the calibration curve previously prepared with narrow PEGs. The MWCO is defined as the molecular weight of PEG with retention of 90%.

Pure water permeability tests

For the measurement of water flow, samples of the membrane were cut in the form of a circle with a surface area of 7.065 cm^2 and loaded in a home-made nanofiltration cell. The deionized water is poured behind the membrane and the nitrogen gas stream with a pressure of 7 Bar was used to provide the driving force. In order to obtain water permeability, the following equation was used:

$$J = Q / t.A$$

In this equation, J is the permeability of water in $L/m^2.h$, Q is the volume of water passed through the membrane in L, A is the active membrane surface in m^2 and t is the time of passage in hours. Rejection percentage of salt, heavy metal or dye was calculated using the following equation:

$$R\% = \left(1 - \frac{C_p}{C_f}\right) \times 100$$

Where C_p and C_f are the concentrations (salt, heavy metal or dye) in permeate and the feed, respectively. The concentration of salt in feed and permeate was evaluated by the conductometer. Three salts, including

Table 2: Composition of polymeric dopes used in the membranes.

Entry	PVDF (wt.%)	NMP(wt.%)	PEG 600 (wt.%)	Hybrid Nanofiber (2 wt.%)
M_1	20	70	10	-
M_2	20	70	10	POM
M_3	20	70	10	TiO_2
M_4	20	70	10	POM/TiO_2
M_5	20	70	10	POM/TiO_2/SiO_2

NaCl and $MgSO_4$ was evaluated (salt concentration in the feed was 0.01 molar, and the applying pressure was 4 bar) the heavy metal rejection was determined using an aqueous solution of $ZnSO_4$ (1000 ppm) and Cd $(NO_3)_2.4H_2O$ (2500 ppm). The concentration of ions in permeate was determined by the conductometer.

In the fouling test, an aqueous solution containing 10 mg/L of Humic Acid (HA) at a pH of 7 was prepared and used as the feed solution in the separation test. The UV-Vis-spectrophotometer measured the HA concentration in the feed, and permeate solution. The rejection was determined according to the above equation. Fouling properties of the prepared membranes have been investigated in our future research work, the initial results show that due to the increased hydrophobic nature of membranes, their fouling resistance has significantly improved.

Stability tests of membranes under UV irradiation

The stability of membranes exposed to the ultraviolet radiation was investigated. Each membrane was cut into several pieces with desired sizes, half of the samples were kept in the dark and the other half was exposed to radiation. The required light source included PHILIPS TL-D 18W BLB 1SL with a λ_{max} at 365 nm. The pure water flux was measured for samples with, and without UV irradiation.

Photocatalytic degradation of Methylene Blue (MB) test

In order to investigate the photocatalytic degradation of MB in the presence of membranes, the aqueous solution of this dye was prepared at a concentration of 10 mg / L and stored in a dark vessel for 10 hours. The fabricated membranes were cut with the same size and immersed in the suitable volume of the aforementioned solution in the separated beakers. The containers were then irradiated with a UV source with two different exposure times (5 and 10 hours). MB degradation was studied by measuring its concentration by UV-Vis spectrophotometer analyses at a wavelength of 664 nm. To survey the effect of light irradiation in the photocatalytic degradation process, sample 5 was stored in MB solution in darkness and after 5 and 10 hours, MB concentration was measured. By comparison with other papers, it was found that the MB degradation rate is comparable to similar work [29-30].

Photocatalytic test for Humic Acid (HA) degradation

Similar to the previous test, a solution of HA was prepared at a concentration of 5 mg/L, and the membrane sample with a surface area of 7.06 cm^2 was placed inside the solution. The degradation of HA in the presence of a UV lamp was studied at intervals of 30 minutes. A UV-Vis spectrophotometry method was applied to determine the HA concentration, and this test was repeated for the membrane with a different composition. As a control sample, membrane 5 was used in the absence of UV light.

RESULTS AND DISCUSSION

Mixed matrix membranes were prepared by incorporation of TiO_2, SiO_2, and MoPOM particles into the PVDF matrix. The photocatalytic activity of these particles has been investigated separately by various researchers [27-32]. However, in the current study, TiO_2, SiO_2, and POM particles were blended by the electrospinning method in a polyvinyl alcohol matrix, and then by removing the polymeric matrix, mineral fibers composed of these particles were fabricated. Thus, photoactivity of the membrane containing the above-mentioned fibers as the additive was surveyed by several tests. Our research group has already proved the suitable performance of the fibers as a catalyst. Characteristics of the applied particle

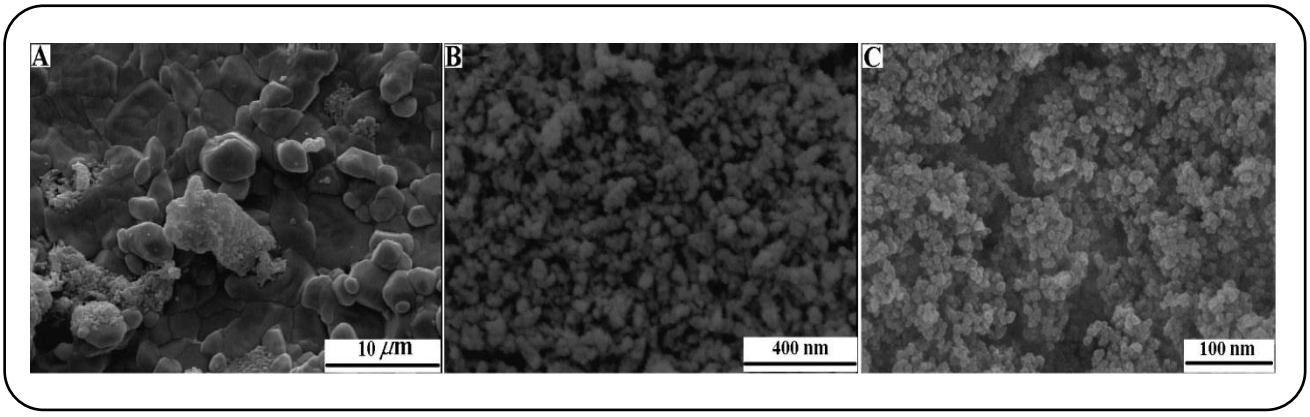

Fig. 1: FESEM images of A: POM, B: TiO_2 and C: SiO_2 .

were examined by some analysis like FESEM, XRD, and the FT-IR. The FESEM images of particles are shown in Fig. 1. As shown in Fig. 1, the POM particles have a nearly cubic shape with dimensions of about 5 µm. In contrast, the TiO_2 and SiO_2 particles are smaller than POM and have dimensions of about 80 to 120 nm and 10 to 20 nm, respectively.

The chemical structure and functional groups of particles, hybrid mineral fibers, pure and mixed matrix membranes are investigated by the FT-IR technique and the related spectra are presented in Fig. 2. In the FT-IR spectra of POM, the characteristic peaks appear at 1618, 1065, 966, 870 cm^{-1} which were attributed to P–O, Mo-O, Mo–O–Mo bonds. Meanwhile, the presence of peaks at 3500 and 1650 cm^{-1} is related to the hydroxyl group and adsorbed water [21, 33]. The characteristic peaks of TiO_2 are usually seen in the range of 400 to 900 cm-1 as a broad peak [34]. A similar interpretation of the spectrum of SiO_2 can also be expressed [35]. The characteristic peaks of mineral hybrid fibers are almost the same as those found in the POM spectrum and this may indicate the absence of chemical interactions between the components. Moreover, the FT-IR spectra of PVDF membrane, and its composites with mineral fibers were brought in Fig. 2. It is clear that the PVDF spectrum has not changed much in the presence of the additive, and only two weak peaks at 300 and 1620 cm^{-1} appear which can confirm the presence of hybrid fibers.

The X-ray diffractograms of TiO_2, SiO_2, POM and hybrid fiber were represented in Fig. 3. As shown, the characteristic peaks of TiO_2, SiO_2 in the related XRD pattern appear at $2\theta = 26$ and 23°, respectively [21, 36]. However, the spectrums of POM, and hybrid fibers are more complicated, although the similarity of these two spectra reveals the entrance of the POM in the structure of hybrid fiber as the main component.

The fibers were prepared by mixing additives and PVA using an electrospinning method. For this purpose, an electric field of 15 kV was used and the distance between the nozzle and collector plate was adjusted to 15 cm and then the composite fibers were calcinated at 500 °C. The FESEM images of the obtained fibers before and after the calcination process is presented in Fig. 4. As it is visibly seen, the diameter of the fiber is quite uniform, and has a maximum of 1 µm and after the destruction of the polymer matrix during the calcination process, mineral fibers were obtained that seemed porous, and could provide a good bed for catalytic activity. Moreover, the fibers containing TiO_2 particles lost their fiber shape after calcifying and were transformed to spindle shape particles in lengths of less than 5 µm. It may be due to phase transformations of TiO_2 particles at high temperatures.

Investigation of surface and cross-sectional morphology of the prepared membranes was carried out using the FESEM method and the results are provided in Fig. 5. The left images that show the surface of the membranes indicate a smooth and constant surface in the PVDF neat membrane (A), while the incorporation of additives into the membrane matrix, increased roughness, and tiny observed nodes was seen probably due to the existence of the hybrid fiber that remained at the surface.

However, in the cross-section of the membranes visible on the right images, the asymmetric structure of the membranes is distinguishable in the form of a top thin dense layer and a lower porous section. It is clear that the thickness of the thin film is higher in the neat PVDF

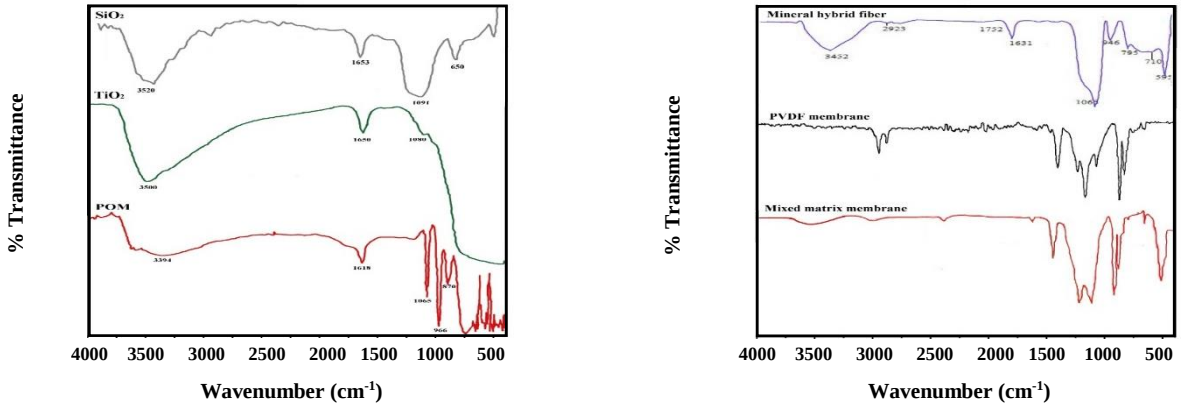

Fig. 2: FT-IR spectra of particles, hybrid fibers, and prepared mixed matrix membrane.

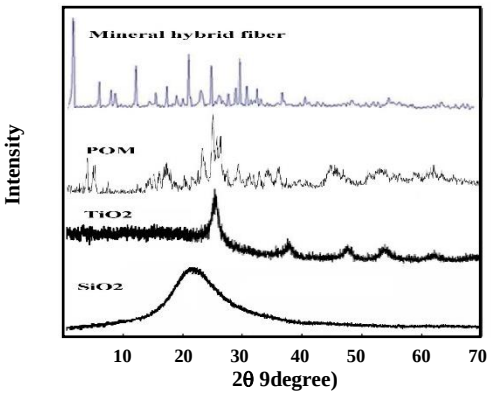

Fig. 3: XRD patterns of particles and hybrid fibers.

membrane and decreases in the composite membranes. Conversely, the observed general trend is the transformation of the sponge-like structure in the pure membrane into the porous finger-like structure in the composite membranes. Meanwhile, the size and number of macro cavities have increased in membranes containing the hybrid fibers and these additives and with a closer look, these particles can be detected in the cross-sections of the membranes.

Molecular weight cut-off

The MWCO is an important parameter which is measured for the membranes and determines the membrane type in terms of its separation capability in the separation of soluble particles, and also is a measure of the pore size of the membrane. The MWCO is calculated by plotting the rejections for each of PEG in the feed solution against related molecular weight and consequently, the rejection above 90 % is recorded as the MWCO [37]. The results for the fabricated membranes are shown in Fig. 6. As can be seen, Membranes containing mineral fibers have a greater MWCO compared with the neat membrane. Among the composite membranes, the membrane M_2, which contains POM particles, has the largest size and membranes M_3, M_4 and M_5 are in the next ranks. However, the obtained MWCO for all membranes is within the range of ultrafiltration. The accuracy and repeatability of the measurements were determined by calculating the Standard Deviation and entered into Fig. 6 and Table 3.

Hydrophilic/hydrophobic nature of the membranes

The surface hydrophilicity of the prepared membranes was evaluated by measuring the contact angle of the water. As shown in Fig. 7, the neat membrane (M1) has a 72˚ water contact angle and in other membranes containing the POM particle, the contact angle is significantly reduced, while the membrane M_3, with TiO_2 duck shape structures, possesses a lower hydrophilicity than membrane M_1 and this can be due to the hydrophobic nature of TiO_2 particles that enter the structure of the membrane. The lowest contact angle belongs to membrane M_2, and M_4 and M_5 membranes exhibit almost similar contact angles.

Pure water flux analysis

To investigate the effect of pressure on the permeability of H_2O from membranes, the Pure Water Flux (PWF) test was performed at three pressures of 5, 7 and 9 bar on the membrane M5 Fig. 8 (A). The results show that by increasing the pressure from 5 to 7 bar, a remarkable increment occurs in the water flux of

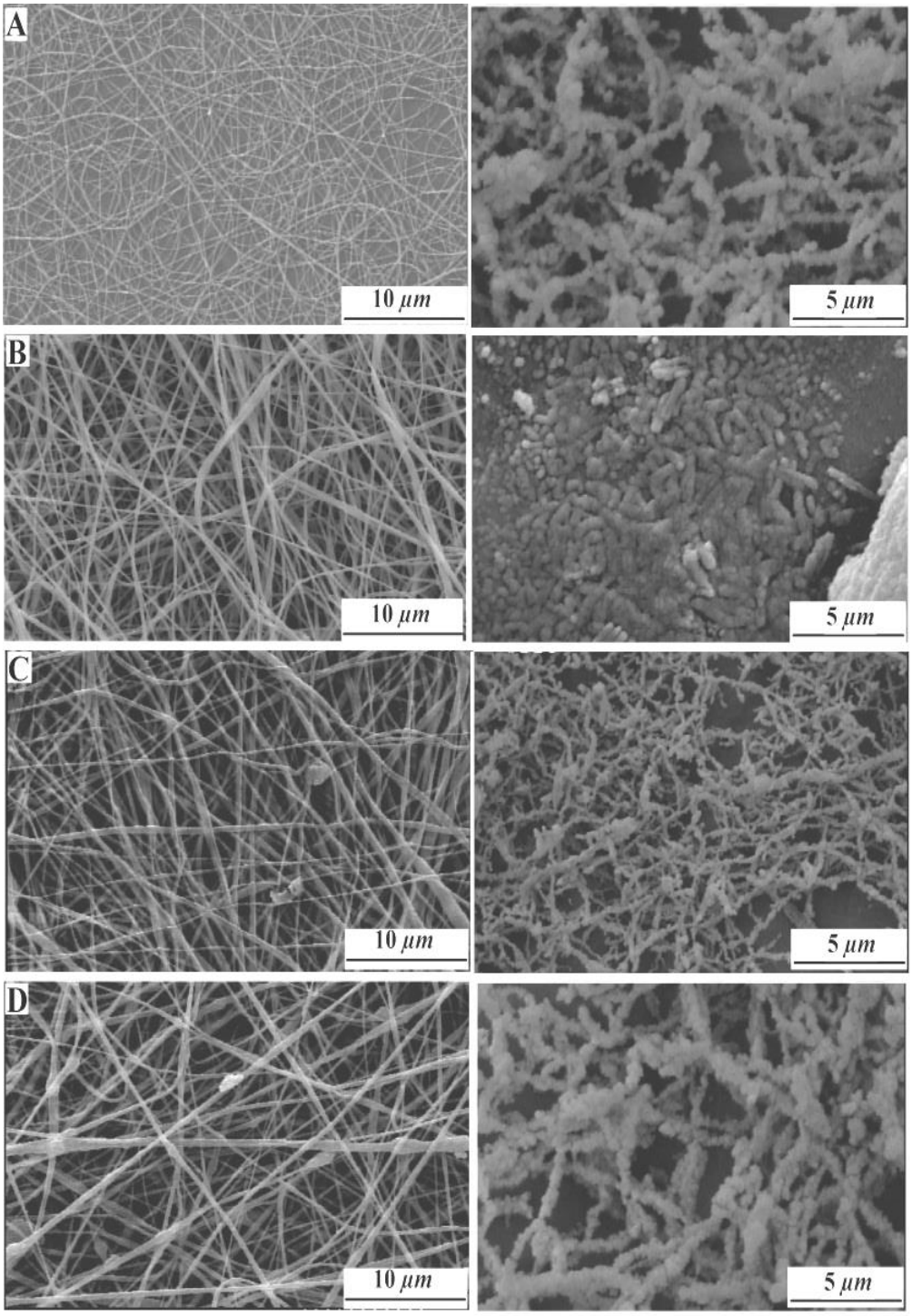

Fig. 4: Prepared fibers before (left) and after (right) calcination, A: POM, B: TiO_2, C: POM/TiO_2, D: POM/TiO_2/SiO_2.

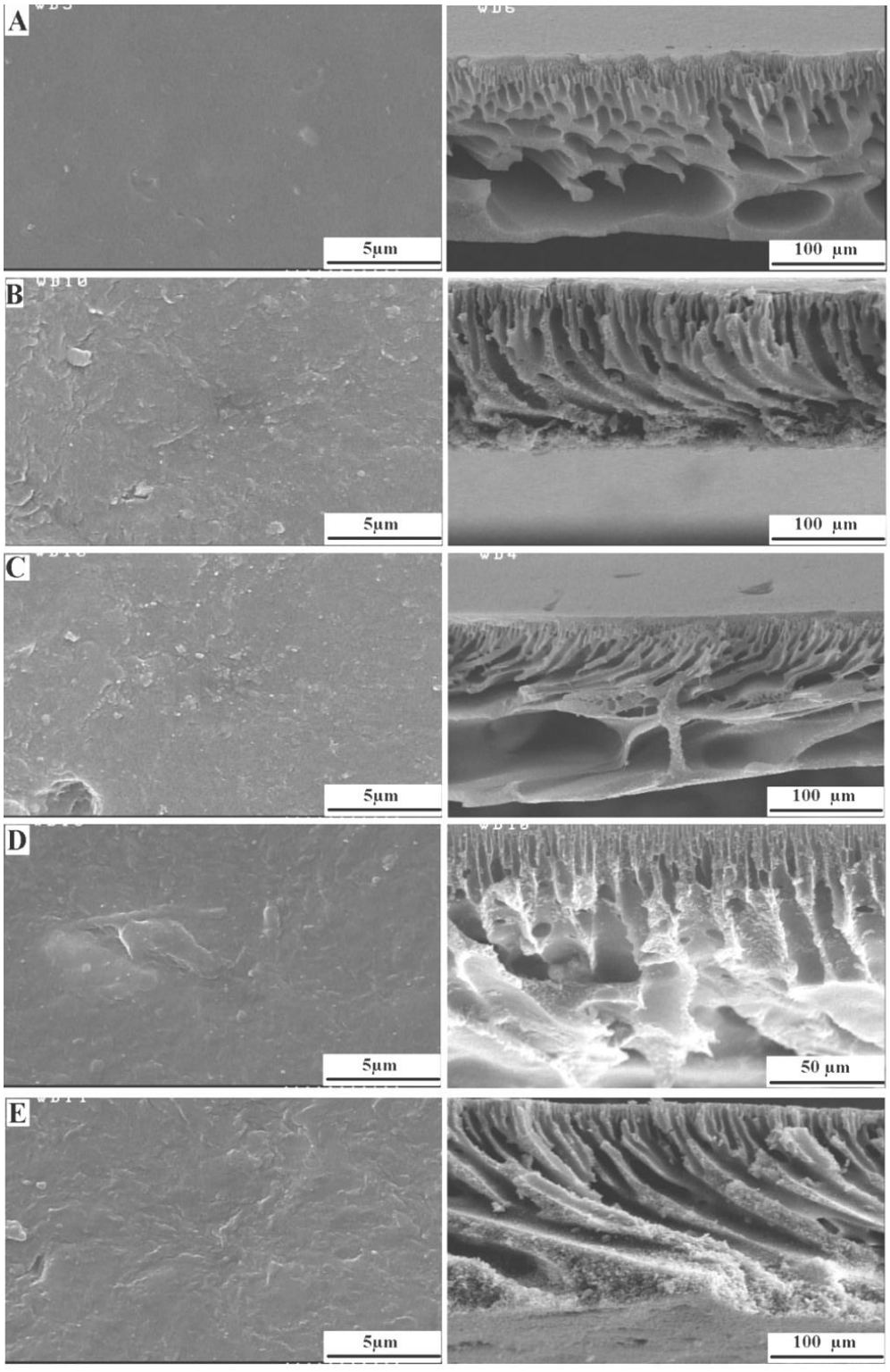

Fig. 5: FESEM images of surface (left) and cross-section (right) of the membranes. A: neat membrane (M1), B: M_2, C:M_3, D:M_4, E:M_5.

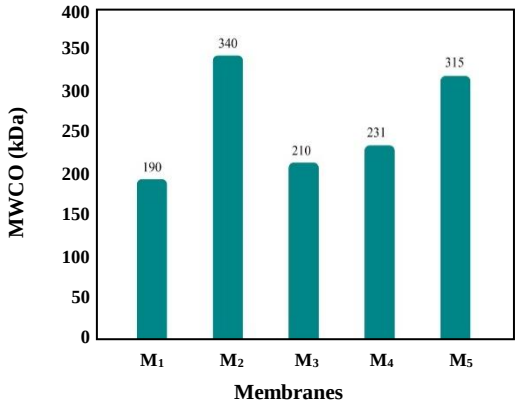

Fig. 6: Results of MWCO for the prepared membranes.

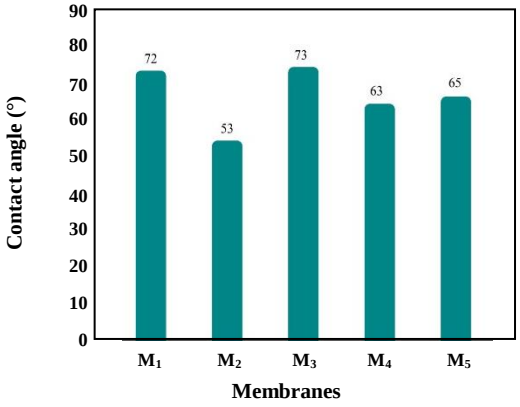

Fig. 7: The Measured water contact angle for the membranes.

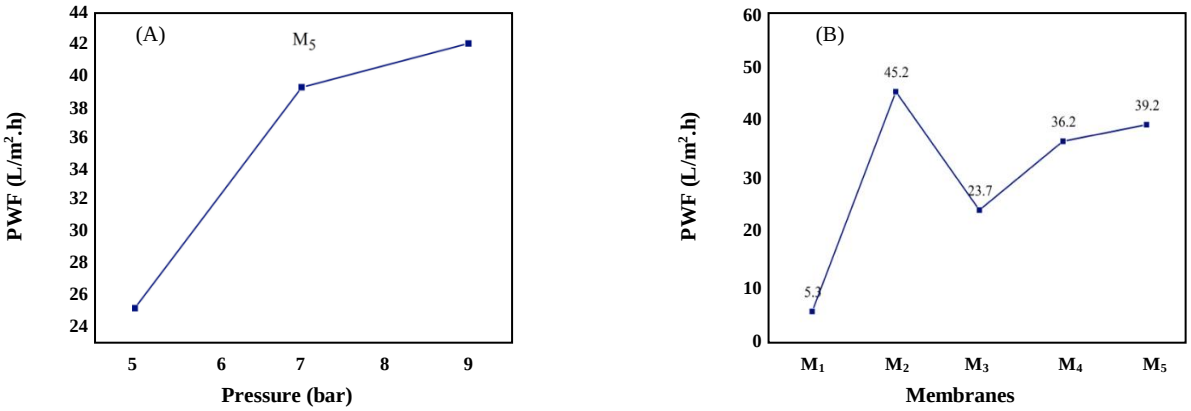

Fig. 8: A) PWF for M5 at different pressures, B) PWFs of the prepared membranes.

the membrane. However, the PWF increase at 9 bar is far lower, probably due to the compressing of membrane pores at high pressures. Therefore, the PWF test for the remaining membranes was carried at five times and is shown in Fig. 8 (B). Clearly, according to the results of previous tests (FESEM and contact angle), composite membranes exhibit a higher PWF, which can be related to the hydrophilic nature of the membranes and, or the increase in the pore size of the membrane due to the addition of mineral fibers.

Stability of the membranes under the irradiation condition

The membranes were exposed to UV irradiation within 48 hours and at 6-hour intervals, the permeability of the membranes was analyzed. As depicted in Fig. 9, for membranes exposed to UV light, permeability has slightly increased over time. It may be due to minor membrane degradation. It was observed that the most significant increase in permeability was related to the TiO_2-containing membranes (M_3, M_4, and M_5), and in the other membranes, it was almost negligible. On the other hand, the tests performed on samples not exposed to irradiation, showed no increase in permeability.

Photocatalytic degradation of MB and HA

In Fig. 10, observations of photocatalytic degradation of MB in a solution containing a piece of the membrane is reported. As it is known, solutions that are in contact with the membrane even before being exposed to UV irradiation, show a drop in the MB concentration due to the adsorption of MB on the membrane [38]. The decreased concentration is less in the neat PVDF membrane, and the rest of the membranes is approximately constant. A decreasing trend can be seen in the MB concentration with increasing irradiation time in solutions containing membranes M_3, M_4, and M_5. The photocatalytic

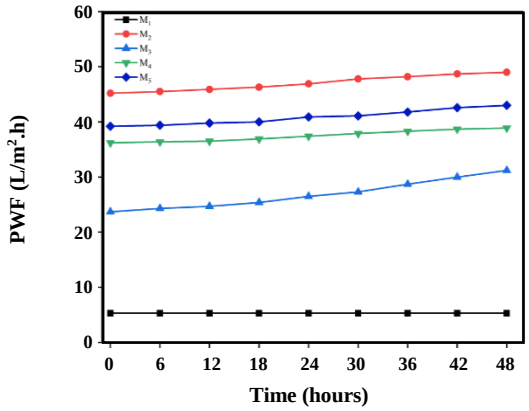

Fig. 9: Stability of membranes under the UV irradiation in term of PWF changes.

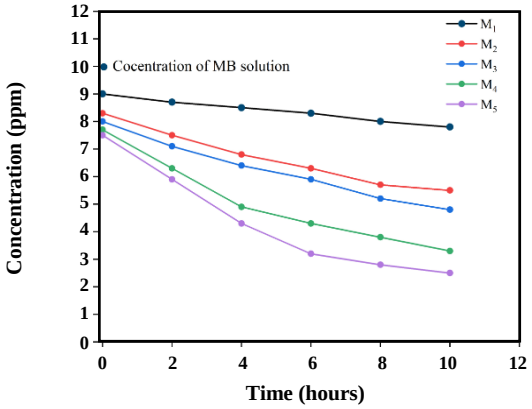

Fig. 10: Photodegradation of MB under the irradiation in the presence of the membranes.

degradation of MB in the presence of membranes can be a logical reason for this observation. However, the degradation in the membranes containing POM, and TiO_2 is much more than the membranes containing each of these particles and the highest rate of degradation is shown in membrane M5 and proves the effect of additives in the photocatalytic degeneration process. Despite the lack of an acceptable justification, this effect was also seen in the study of the photocatalytic activity of mineral hybrid fibers. It should be noted that the membrane M5 in the absence of UV light did not show any photocatalytic activity [39, 40].

For further investigation of the efficiency of the prepared membranes, the photocatalytic elimination of HA was studied. The results are tabulated in Table 3. In this test, it is also observed that in the absence of UV irradiation, membranes only cause a slight decrease in the concentration of HA, which is related to the absorption of this material on the membrane. Meanwhile, the most considerable photocatalytic removal rate is seen in the M_5 membrane, and the other composite membranes exhibit much better performance than the neat PVDF membrane. On the other hand, removal of HA is carried out using membranes by a rejection test set-up and, as shown in Table 3, membranes containing hybrid fibers show a higher removal efficiency despite increasing the PWF. In comparison to the other reported papers, it was found that the reported MB degradation rate is comparable to them. However, the reported results for HA were related to the third hour of analysis and seemed to have an acceptable performance. Furthermore, these membranes have the potential to be used in photocatalytic degradation tests during feed passing through the membrane [41, 44].

Rejection of salts and heavy metals

In order to study the performance of membranes made for the removal of salts, and heavy metals, several salts and heavy metals were utilized in the rejection test and the results are presented in Table 3. It was observed that composite membranes, despite having larger pores, indicate significantly improved performance in the separation of these materials, and therefore can be used potentially for desalination of water or sewage treatment.

The molecular weight of HA is about 227 g/mol which is smaller than MWCO of most membranes. Moreover, low HA rejection may be due to its molecular penetration through the membrane. It should be noted that the membrane test method is a dead-end system, and if the circular system is used, the efficiency would be much higher. On the other hand, for HA, the reported results were related to the third hour of analysis.

CONCLUSIONS

PVDF mixed matrix membranes were fabricated by incorporation of TiO_2 / SiO_2 / POM hybrid fibers into the polymeric dope solution to give them photocatalytic activity. Initially, hybrid fibers were synthesized by electrospinning and calcination techniques and then these additives were entered into the membrane matrix. The FESEM reveals that the average diameter of the hybrid composite fibers is about 500 nm. Furthermore, membrane morphology was examined by FESEM. The properties

Table 3: HA, salts and heavy metal rejection efficiency by different membranes.

Membranes	HA degradation using membrane (%)	Rejection of HA (%)	Salt rejection (%)	Heavy metal removal (%)
M_1	10±0.5	25±1.3	$MgSO_4$: 34.2±1.2	Zn^{2+}: 30±0.8
			NaCl: 25.6±0.9	Cd^{2}: 29±1.3
M_2	30±0.8	32±2.1	$MgSO_4$: 58±1.1	Zn^{2+}: 49.2±1.6
			NaCl: 47±0.8	Cd^{2+}: 46.8±1.3
M_3	46.2±0.6	45±1.9	$MgSO_4$: 39.2±1.3	Zn^{2+}: 45±0.9
			NaCl: 37.5±0.7	Cd^{2+}: 42.9±1.4
M_4	79.3±0.7	49±2.5	$MgSO_4$: 42.6±1.5	Zn^{2+}: 47.3±1.1
			NaCl: 40.1±0.9	Cd^{2+}: 44.8±0.8
M_5	89.8±0.6	51±1.1	$MgSO_4$: 62±1.2	Zn^{2+}: 51±1.3
			NaCl: 51±1.4	Cd^{2+}: 48±1.5

of the prepared photocatalytic membrane were examined by several investigates such as pure water flux, contact angle, salt, and heavy metal rejection. Photocatalytic experiments confirm that membranes exhibit highly efficient and as expected, the membranes containing hybrid fibers showed the best performance. M5 membrane, which contained POM/TiO_2/SiO_2 hybrid fibers, had the best performance in photocatalytic activity.

Received : Jul. 27, 2019 ; Accepted : Nov. 4, 2019

REFERENCES

[1] Kobielska P.A., Howarth A.J., Farha O.K., Nayak S., Metal-Organic Frameworks for Heavy Metal Removal from Water, *Coordination Chemistry Reviews* **358**: 92-107 (2018).

[2] Lu F., Astruc D., Nanomaterials for Removal of Toxic Elements from Water, *Coordination Chemistry Reviews* **356**: 147-164 (2018).

[3] Natarajan S., Bajaj H.C., Tayade R.J., Recent Advances Based on the Synergetic Effect of Adsorption for Removal of Dyes from Waste Water Using Photocatalytic Process, *Journal of Environmental Sciences* **65**: 201-222 (2018).

[4] Changming D., Chao S., Gong X., Ting W., Xiange W., Plasma Methods for Metals Recovery from Metal–Containing Waste, *Waste Management* **77**: 373-387 (2018).

[5] Rahman M.T., Kameda T., Kumagai S., Yoshioka T., A Novel Method to Delaminate Nitrate-Intercalated MgAl Layered Double Hydroxides in Water and Application in Heavy Metals Removal from Waste Water, *Chemosphere* **203**: 281-290 (2018).

[6] Taseidifar M., Makavipour F., Pashley R.M., Rahman A.F.M.M., Removal of Heavy Metal Ions from Water Using Ion Flotation, *Environmental Technology & Innovation* **8**: 182-190 (2017).

[7] Sharifi Aliabadi R., Mahmoodi N.O., Synthesis and Characterization of Polypyrrole, Polyaniline Nanoparticles and Their Nanocomposite for Removal of azo Dyes; Sunset Yellow and Congo Red, *Journal of Cleaner Production* **179:** 235-245 **(**2018).

[8] Belletire J.L., Mahmoodi N.O., Efficient Microscale Filtration, *Journal of Chemical Education*, 964 (1989) 11.

[9] Lian J.-Z., Tsai C.-T., Chang S.-H., Lin N.-H., Hsieh Y.-H., Iron Waste as an Effective Depend on TiO_2 for Photocatalytic Degradation of Dye Waste Water, *Optik - International Journal for Light and Electron Optics* **140**: 197-204 (2017).

[10] Zatloukalová K., Obalová L., Kočí K., Čapek L., Matěj Z., Šnajdhaufová H., Ryczkowski J., Słowik G., Photocatalytic Degradation of Endocrine Disruptor Compounds in Water over Immobilized TiO_2 Photocatalysts, *Iran. J. Chem. Chem. Eng. (IJCCE)*, **36(2)**: 20-38 (2017).

[11] Chakraborty S., Loutatidou S., Palmisano G., Kujawa J., Mavukkandy M.O., Al-Gharabli S., Curcio E., Arafat H.A., Photocatalytic Hollow Fiber Membranes for the Degradation of Pharmaceutical Compounds in Wastewater, *Journal of Environmental Chemical Engineering* **5**: 5014-5024 (2017).

[12] Teow Y.H., Ooi B.S., Ahmad A.L., Study on PVDF-TiO_2 Mixed-Matrix Membrane Behaviour Towards Humic Acid Adsorption, *Journal of Water Process Engineering* **15**: 99-106 (2017).

[13] Zhao Ma Y., L., Chang W., Huang Z., Feng X., Qi X., Li Z., Efficient Photocatalytic Degradation of Gaseous *N*,*N*-dimethylformamide in Tannery Waste Gas Using Doubly Open-Ended Ag/TiO_2 Nanotube Array Membranes, *Applied Surface Science* **444**: 610-620 (2018).

[14] Nair A.K., JagadeeshBabu P.E., Ag-TiO_2 Nanosheet Embedded Photocatalytic Membrane For Solar Water Treatment, *Journal of Environmental Chemical Engineering* **5**: 4128-4133 (2017).

[15] Janitabar Darzi S ., Movahedi M ., Visible Light Photodegradation of Phenol Using Nanoscale TiO_2 and ZnO Impregnated with Merbromin Dye: A Mechanistic Investigation, *Iran. J. Chem. Chem. Eng. (IJCCE),* **33(2)**: 55-64 (2014)

[16] Zayadi R.A., Bakar F.A., Comparative Study on the Performance of Au/F-TiO_2 Photocatalyst Synthesized from Zamzam Water and Distilled Water under Blue Light Irradiation, *Journal of Photochemistry and Photobiology A: Chemistry* **346**: 338-350 (2017).

[17] Shi H., Yu Y., Zhang Y., Feng X., Zhao X., Tan H., Khan S.U., Li Y., Wang E., Polyoxometalate/TiO_2/Ag Composite Nanofibers with Enhanced Photocatalytic Performance under Visible Light, *Applied Catalysis B: Environmental* **221**: 280-289 (2018).

[18] Li Y., Zhou J., Fan Y., Ye Y., Tang B., Preparation of Environment-Friendly 3D Eggshell Membrane-Supported Anatase TiO_2 as a Reusable Photocatalyst for Degradation of Organic Dyes, *Chemical Physics Letters* **689**: 142-147 (2017).

[19] Li S., Zhang L., Zhao C., Yu Y., Zhang Z., Li L., A New Polyoxometalate-Based Helical Compound with Entanglement Nodes: Structure, Electrocatalytic and Photocatalytic Properties, *Journal of Molecular Structure* **1145**: 76-80 (2017).

[20] Zhang L., Mi T., Ziaee M.A., Liang L., Wang R., Hollow POM@MOF Hybrid-Derived Porous Co_3O_4/$CoMoO_4$ Nanocages for Enhanced Electrocatalytic Water Oxidation, *Journal of Materials Chemistry A* **6:** 1639-1647 (2018).

[21] Yu L., Ding Y., Zheng M., Polyoxometalate-Based Manganese Clusters as Catalysts for Efficient Photocatalytic and Electrochemical Water Oxidation, *Applied Catalysis B: Environmental* **209**: 45-52 (2017).

[22] Fallah Shojaei A., Loghmani M.H., Effect of Microwave Irradiation on Morphology and Size of Anatase Nano Powder: Efficient Photodegradation of 4-Nitrophenol by W-doped Titania, *Bulletin of the Korean Chemical Society*, **33**: 3981-3986 (2012).

[23] Tan W., Luo L., Zheng Y., Jegatheesan V., Shu L., Zhang S., Yang M., Wang H., Preparation and Photocatalytic Activity of Heteropolyacid Salt (POM)/TiO_2 Composites Synthesized by Solid Phase Combustion Method, *Process Safety and Environmental Protection* **104**: 558-563 (2016).

[24] Shojaei A.F., Rezvani M.A., Loghmani M.H., Comparative Study on Oxidation Desulphurization of Actual Gas Oil and Model Sulfur Compounds with Hydrogen Peroxide Promoted by Formic Acid: Synthesis and Characterization of Vanadium Containing Polyoxometalate Supported on Anatase Crushed Nanoleaf, *Fuel Processing Technology* **118**: 1-6 (2014).

[25] Liu C., Zhang Z., Liu W., Du X., Liu S., Cui Y., Synergistic Effect Of Polyoxometalate Solution and TiO_2 Under UV Irradiation To Catalyze Formic Acid Degradation and their Application in the Fuel Cell and Hydrogen Evolution, *Green Energy & Environment* **2:** 436-441 (2017).

[26] Subramaniam M.N., Goh P.S., Lau W.J., Ng B.C., Ismail A.F., AT-POME Colour Removal Through Photocatalytic Submerged Filtration Using Antifouling PVDF-TNT Nanocomposite Membrane, *Separation and Purification Technology* **191:** 266-275 (2018).

[27] Dehghan Niri A., Faridi-Majidi R., Saber R., Khosravani M., Adabi M., Electrospun Carbon Nanofiber-Based Electrochemical Biosensor for the Detection of Hepatitis B Virus, *Biointerface Research in Applied Chemistry*, **9(4)**: 4022-4026 (2019).

[28] Sobhanipour M.A., Karimikan R ., Khodabakhshi M., Nitrate Removal from Water Using TiO_2/ PVDF Membrane Photobioreactor, *Iran. J. Chem. Chem. Eng. (IJCCE)*, (2019). [In Press].

[29] Xu H., Ding M., Chen W., Li Y., Wang K., Nitrogen-Doped GO/TiO2 Nanocomposite Ultrafiltration Membranes for Improved Photocatalytic Performance, *Separation and Purification Technology* **195**: 70-82 (2018).

[30] Xu M., Bi B., Xu B., Sun Z., Xu L. , Polyoxometalate-Intercalated ZnAlFe-Layered Double Hydroxides for Adsorbing Removal and Photocatalytic Degradation of Cationic Dye, *Applied Clay Science* **157**: 86-91 (2018).

[31] Xing Z., Zhang J., Cui J., Yin J., Zhao T., Kuang J., Xiu Z., Wan N., Zhou W., Recent Advances in Floating TiO_2-Based Photocatalysts for Environmental Application, *Applied Catalysis B: Environmental* **225:** 452-467 (2018).

[32] Taghavi M., Tabatabaee M., Ehrampoush M.H., Ghaneian M.T., Afsharnia M., Alami A., Mardaneh J., Synthesis, Characterization and Photocatalytic Activity of TiO_2/ZnO-Supported Phosphomolybdic Acid Nanocomposites, *Journal of Molecular Liquids* **249:** 546-553 (2018).

[33] Adabi M., Saber R., Adabi M., Sarkar S., Examination of Incubation Time of Bare Gold Electrode Inside Cysteamine Solution for Immobilization of Multi-Walled Carbon Nanotubes on A Gold Electrode Modified with Cysteamine, *Microchim Acta* **172**: 83–88 (2011).

[34] Choksumlitpol P., Mangkornkarn C., Sumtong P., Onlaor K., Eiad-ua A., Fabrication of Anodic Titanium Oxide (ATO) for Waste Water treatment Application, *Materials Today: Proceedings* **4:** 6124-6128 (2017).

[35] Delsouz Khaki M.R., Shafeeyan M.S., Raman A.A.A., Daud W.M.A.W., Evaluating the Efficiency of Nano-Sized Cu Doped TiO_2/ZnO Photocatalyst Under Visible Light Irradiation, *Journal of Molecular Liquids* **258**: 354-365 (2018).

[36] Lavorato C., Argurio P., Mastropietro T.F., Pirri G., Poerio T., Molinari R., Pd/TiO2 Doped Faujasite Photocatalysts for Acetophenone Transfer Hydrogenation in a Photocatalytic Membrane Reactor, *Journal of Catalysis* **353:** 152-161 (2017).

[37] Karaolia P., Michael-Kordatou I., Hapeshi E., Drosou C., Bertakis Y., Christofilos D., Armatas G.S., Sygellou L., Schwartz T., Xekoukoulotakis N.P., Fatta-Kassinos D., Removal of Antibiotics, Antibiotic-Resistant Bacteria and Their Associated Genes by Graphene-Based TiO_2 Composite Photocatalysts under Solar Radiation in urban Wastewaters, *Applied Catalysis B: Environmental* **224:** 810-824 (2018).

[38] Wu C-H, Chern J-M., Kinetics of Photocatalytic Decomposition of Methylene Blue, *Ind. Eng. Chem. Res.* **45**: 6450-6457 (2006).

[39] Avramidou K.V., Zaccheria F., Karakoulia S.A., Triantafyllidis K.S., Ravasio N., Esterification of Free Fatty Acids Using Acidic Metal Oxides and Supported Polyoxometalate (POM) Catalysts, *Molecular Catalysis* **439:** 60-71 (2017).

[40] Dzinun H., Othman M.H.D., Ismail A.F., Puteh M.H., Rahman M.A., Jaafar J., Stability Study of PVDF/TiO2 dual-layer hollow Fiber Membranes under Long-Term UV Irradiation Exposure, *Journal of Water Process Engineering* **15:** 78-82 (2017).

[41] Dui X.-J., Wu X.-Y., Liao J.-Z., Teng T., Wu W.-M., Yang W.-B., Photocatalytic Properties of Two POM-Templated Organic-Inorganic Hybrid Compounds, *Inorganic Chemistry Communications* **56**: 112-115 (2015).

[42] Rahimpour A., Jahanshahi M., Mollahosseini A., Rajaeian B., Structural and Performance Properties of UV-Assisted TiO2 Deposited Nano-Composite PVDF/SPES Membranes, *Desalination* **285:** 31-38 (2012).

[43] Simone S., Galiano F., Faccini M., Boerrigter M. E., Chaumette C., Drioli E., Figoli A., Preparation and Characterization of Polymeric-Hybrid PES/TiO_2 Hollow Fiber Membranes for Potential Applications in Water Treatment, *Fibers*, **5**: 14-33 (2017); doi:10.3390/fib5020014

[44] Liu Y., Xiao T., Bao C., Zhang J., Yang X., Article Performance and Fouling Study of Asymmetric PVDF Membrane Applied in the Concentration of Organic Fertilizer by Direct Contact Membrane Distillation (DCMD, *Membranes*, **8**: 9-22 (2018).